Hindawi
Advances in Materials Science and Engineering
Volume 2018, Article ID 3489720, 8 pages
https://doi.org/10.1155/2018/3489720

Research Article

Influence of Energy State of Montmorillonite Interlayer Cations on Organic Intercalation

Limei Wu,[1] **Shiyue Cao**,[1] **and Guocheng Lv**[2]

[1]*School of Materials Science and Engineering, Shenyang Jianzhu University, Shenyang 110168, China*
[2]*Beijing Key Laboratory of Materials Utilization of Nonmetallic Minerals and Solid Wastes, National Laboratory of Mineral Materials, School of Materials Science and Technology, China University of Geosciences, Beijing 100083, China*

Correspondence should be addressed to Limei Wu; lmwu@sjzu.edu.cn and Guocheng Lv; guochenglv@cugb.edu.cn

Received 11 August 2018; Accepted 24 October 2018; Published 13 November 2018

Academic Editor: Marino Lavorgna

It is well known that the intercalation of montmorillonite (Mt) with organic cations is a fast process. During the intercalation, the interaction between the original cations and the structure layer of Mt keeps changing, and the basal spacing of Mt keeps increasing until an organic environment has been built in the interlayer. Many properties of Mt also change during the intercalation, such as hydrophobic or hydrophilic property and thermal stability. In this research, the impact of intercalation on the properties of Mt was studied by investigating the change in basal spacing and energy that coordinates the interlayer cations during the intercalation of Mt with organic cations. The interaction between interlayer cations and the layers in the Mt structure and the change in the system energy were obtained by using molecular dynamics simulation. All the experiment and calculation results provide a theoretical proof in organic intercalation mechanism.

1. Introduction

Clay minerals have a wide range of properties, which make them important to the earth sciences, engineering, and industry. Clay minerals have a layered structure at the nanoscale, and each layer consists of some combinations of two layer types with silicon tetrahedra and aluminum octahedra as basic units [1, 2]. Due to the positive charge, the interlayer cations can interact through electrostatic interactions with the silicon tetrahedral [3]. Mt is a layered aluminosilicate with negatively charged layers compensated by cations such as Na^+ (Na-Mt) and Ca^{2+} (Ca-Mt). The cations can be exchanged by suitable ions or polymers [4]. Numerous previous studies have focused on the characterization of alkyl ammonium cations arrangement and conformation after intercalation in the interlayer of layered silicates [5–7]. The structure of the surfactant (e.g., chain length, number of long chains, and head group) and the intrinsic properties of the original clay material have a combined effect on the structure and properties of the resultant organoclay [5, 8, 9]. Until now, only few studies on the organic intercalation mechanism have been reported. And the researches in organic intercalation of Mt are not systematic, which have not resolved the essential problems [10, 11].

However, the secondary driving forces include hydrophobicity of organic cations, intermolecular repulsion, diffusion of interlayer cations, Van der Waals force [7, 12]. As the amount of organic cations in the interlayer increases, arrangement of interlayer cations is gradually changed from monolayer paralleled to bilayer paralleled or bilayer paralleled and monolayer tilt [9, 13]. Structures of organic cations (chain length and functional groups) and its interaction with Mt have influences on structure and performance of organic Mt [12, 14]. Many researchers' characterized arrangement and conformation of alkyl ammonium cations intercalated Mt. Stacking density of alkyl ammonium cations, amount of intercalated cations, leads to variations of interlayer arrangement [15] and spacing of Mt. The remarkable development of molecular computer simulations is very helpful in demonstrating a chemical evolution on the structure and behavior of clay minerals on the atomic level. Molecular

modeling (MD) has been widely used to study the interlayer structural characteristics of clay minerals from atomic-level insights on the structural features of the system [16–19]. MD simulations methods were also employed to study the microscopic aspects of the interaction of organic cations with the Mt surface, and the methods could obtain the interaction energy and work of adhesion [20–26].

In montmorillonite crystal structure, aluminum ions in aluminum-oxygen octahedron are easily replaced by various ions such as magnesium or iron, while the silicon ions in silicon-oxygen are easily replaced by aluminum. Meantime, cations like Na^+ or Ca^{2+} can be filled into the interlayer space to balance the charge, ascribed to the weak interaction force, such as Van de Waals force, between them. Cations in the interlayer of Mt, such as Na^+ and Ca^{2+}, are hydrated, so the spacing of Mt is actually a function of water content. With different types of interlayer cations, the distribution, hydration, and diffusion properties in the interlayer of Mt are different [27–30]. Only few researchers reported the relative position relation of interlayer cations and replaced Mg^{2+} [31–34], and it is hard to explain this microscopic issue by experimental methods. Furthermore, as there are exchangeable cations in the Mt interlayer space, it is easy for organic intercalation process to get organic Mt. Some organic Mt can be applied to medicine, paint, drilling fluid, etc [35], which will greatly expand the application of Mt. However, as the process of organic cations intercalating Mt is the interaction of multiple forces, the research and description on intercalation process and mechanism are not clear. The researchers did not focus on interaction force between layer and interlayer cations [36]. To solve the process of organic intercalation, it is an effective method to use molecular dynamic simulation through the simple model to fundamental interactions between organic monomers and Mt.

In this paper, the mechanism of Mt intercalation with organic cations and properties of organic modified Mt were studied by investigating the energy change and the order in which cations were exchanged in the process of Mt intercalation with butylimidazole chlorides. XRD and TG-DTA were undertaken to characterize the change in basal spacing and thermal stability of Mt. Numerous previous studies have focused on the characterization of 1-butyl-3-methylimidazolium chloride monohydrate (C_4mimCl) arrangement and conformation after intercalation in the interlayer of layered silicates. The aim of the experiment is to study the position of Mg replacing Al in the Mt octahedron and interaction with interlayer Na^+ in detail. The interaction between Na^+ and silicon-oxygen tetrahedron will affect the intercalation of organic cations.

2. Materials and Methods

2.1. Materials. The Mt obtained from the Clay Mineral Repositories in Purdue University (West Lafayette, IN) was used without further purification. It has a chemical formula of $(Ca_{0.12}\ Na_{0.32}\ K_{0.05})[A_{l3.01}\ Fe(III)_{0.41}\ Mg_{0.54}][Si_{7.98}\ Al_{0.02}]O_{20}(OH)_4$, a CEC of 85 ± 3 $mmol_c/100$ g [37], a layer charge of 0.32 eq/mol per $(Si,Al)_4O_{10}$ [38], an external surface area (ESA) of 23 m^2/g, respectively [5], and a mean particle size of 3.2 μm with a d_{25} to d_{75} in the range of 3–10 μm.

1-Butyl-3-methylimidazolium chloride monohydrate (CAS#: 79917-90-1, C_4mimCl) was obtained from Shanghai Darui Finechemical Co. Ltd. (Shanghai, China). They have pKa values of 7.08 ± 0.1 due to protonation of both nitrogen atoms.

2.2. Methods. For C_4mimCl intercalation into the Mt interlayer, a desired amount of C_4mimCl was dissolved in 100 mL of distilled water followed by the addition of 0.5 g of synthetic Mt. The mixtures were stirred at 40°C for 6 h. After the mixtures were centrifuged at 10000 rpm for 20 min, the supernatants were filtered through syringe filters with the size of 0.22 μm before being analyzed for equilibrium C_4mimCl concentrations. The final solid products were washed six times with deionized water and dried at 65°C.

Powder XRD analyses were performed on a Rigaku D/max-III a diffractometer (Tokyo, Japan) with a Ni-filtered Cu Kα radiation at 30 kV and 20 mA. Orientated samples were scanned from 3° to 10° at 2°/min with a scanning step of 0.01°. Powder samples were packed in horizontally held trays. The changes in the XRD peak positions reflect the intercalation of the organic cations into layered silicates. The Bragg equation was applied to calculate the basal spacing of Mt platelets. The gallery sizes in intercalated hybrids were deduced from XRD peak positions of (001) of the hybrids.

Thermogravimetric (TG) analyses were carried out on TGA Q-500 (TA Instruments, New Castle, USA) from room temperature to 800°C, at a heating rate of 10°C/min under a nitrogen flow of 60 ml/min. TG curves were used to determine the percentage of weight loss [32]. Differential scanning calorimetry (DSC) was performed using a differential scanning calorimeter (TA Instruments Q100) fitted with a cooling system using liquid nitrogen. It was calibrated with an indium standard. Samples of 6 mg Mt were accurately weighed into aluminum pans and sealed and then heated from 30 to 800°C at 10°C/min under a nitrogen flow of 60 ml/min.

Molecular simulation was performed using the module "CASTEP" of Materials Studio 6.0 software to investigate the sorption sites of C_4mimCl on Mt. The primitive unit cell of Mt was optimized with the generalized gradient approximation (GGA) for the exchange-correlation potential (PW91) which is appropriate for the relatively weak interactions present in the models studied. The resulting primitive unit cell was expressed by the parameters a = 15.540 Å, b = 17.940 Å, c = 12.56 Å, and $\alpha = \gamma = 90°$, $\beta = 99°$. Based on the primitive unit cell, a series of (3 × 2 × 1) supercells were built with the spacing of layers set to 12.34 Å, 12.72 Å, 13.11 Å, and 13.43 Å, respectively. To investigate the intercalating mechanism of C_4mimCl in the pure Mt layer, a simulated annealing algorithm was used to perform canonical Monte Carlo (MC) simulation with C_4mimCl as adsorbed on the layer of pure Mt. For the grafted (the interaction force with Mt layer) Mt, MC simulation was conducted with C_4mimCl as adsorbed. The number of cycles is set to 3, and the step of one cycle is 10^6, a representative part of the interface devoid of any arbitrary boundary effects.

All the bonded terms were calculated based on CVFF, except for the OH bond and angles in the clay framework which were calculated from CLAYFF. The temperature was set at 298 K, and time was 1 ns with a time step of 1 fs. The data were collected on the last 200 ps for later analyses. Based on the structure of the preferential adsorption model of C_4mimCl in the layer of Mt predicted by MC calculation, GGA-PW91 was used to optimize the structure again and to predict the interaction energy between C_4mimCl and Mt layer to a greater accuracy. All of the GGA-PW91 calculations were performed using a double numerical plus polarization (DNP)function as the basis set and density functional theory-dispersion (DFT-D) correction. So for all calculations, the heavy atoms of Mt were frozen, whereas the hydrogen of Mt and C_4mimCl molecules were fully relaxed.

3. Results

3.1. Properties of Na-Mt and C_4-Mt. The nature of organic intercalation is exchanging the interlayer cation of Mt with the organic cation, and the process is affected by the energy of the interlayer cation. Intercalating Mt with C_4minCl solution of 50, 200, and 1000 mg/L was used to obtain organic Mt samples C_4-Mt-1, C_4-Mt-2, and C_4-Mt-3. The interlayer spacing value of Mt varies with different intercalation concentrations (Figure 1), and the value increased from 12.34 Å to 13.0 1 Å (50 mg/L) and 13.65 Å (200 mg/L) and finally reached 14.25 Å with the C_4minCl solution of 1000 mg/L. (001) crystal face diffraction peaks of intercalated Mt are sharp and narrow, indicating that the interlayer C_4minCl is well distributed and stable in Mt gallery.

The results demonstrates that the organic cation with different initial concentrations leading to organic Mt with various interlayer spacing is related to the intercalation amount and the arrangement of interlayer organic cations. Previous works also showed that organic cations entered Mt gallery by ion exchange, and different organic intercalation amounts imply different amounts of inorganic cations exchanged, among which some cations exchanged firstly and some later [39, 40].

The TG curves of Na-Mt and C_4-Mt (Figure 2(a)) shows obvious distinctions in weight loss curves of Na-Mt and organic intercalated Na-Mt. At the range of 50 to 200°C, Na-Mt has a weight loss of 2.5%, owing to detachment of interlayer water and adsorbed water. The weight loss decreased as the intercalation amount increased, and the weight loss of C_4-Mt-1, C_4-Mt-2, and C_4-Mt-3 at 50–200°C are 2%, 1.5%, and 1%, respectively. These samples are with the same Mt structure, and the adsorbed water amount is similar. Therefore, the difference in weight loss is mainly ascribed to the loss of different interlayer binding water amounts of the three samples, and more interlayer organic cations lead to a less binding water amount. Then at the range of 300 to 500°C, no weight loss of Na-Mt was observed, while 8%, 11%, and 12% weight loss of C_4-Mt-1, C_4-Mt-2, and C_4-Mt-3 occurred, indicating interlayer C_4min^+ decomposed and more interlayer C_4min^+ resulting in greater loss. From 500 to 700°C, both C_4-Mt and Na-Mt have weight loss of 5%, owing to decomposition of structural water.

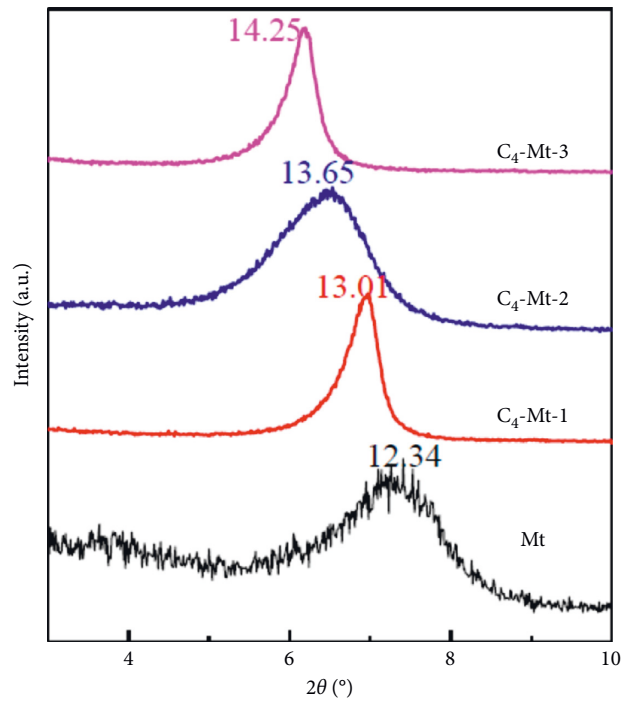

Figure 1: X-ray diffraction patterns of montmorillonite intercalated with C_4mimCl (d/Å).

In general, Mt has two major endothermic peaks (Figure 2(b)). The first one occurred at 80–250°corresponding to evaporation of absorbed water and water that coordinates interlayer cations. The second peak can be observed at 600–700°C due to the loss of the structural hydroxyl group. Obvious differences can be found between the DTA curves of C_4-Mt (red) and Na-Mt (blue) too. For Na-Mt, there are two endothermic peaks as the temperature increases: (1) the peak corresponds to the loss of absorbed surface water and water in the interlayer at 80°C; (2) the peak corresponds to the loss of the structural hydroxyl group at 650°C, which causes structural distortion without amorphization. The first endothermic valley (50–200°C) of C_4-Mt-1, C_4-Mt-2, and C_4-Mt-3 locates in higher temperature than first endothermic valley of Na-Mt, indicating that the endothermic valley increased as the intercalation amount increased. The second endothermic valley (300–500°C) also increased along with the intercalation amount due to decomposition of organic cations.

In summary, organic cations enter gallery by ion exchange mechanism, and inorganic are not being exchanged at the same time but one after the other. Stability of interlayer organic cations are different, leading to diverse decomposition temperatures. Molecular dynamics simulation was carried out to explain the energy of interlayer inorganic cations and exchange and intercalation process of organic cations.

3.2. Molecular Simulation of Na-Mt. Basal spacing of Na-Mt was 12.34 Å (Figure 1). As the charge-balancing cation, Na^+ in the interlayer of Mt tends to hydrate with water molecule,

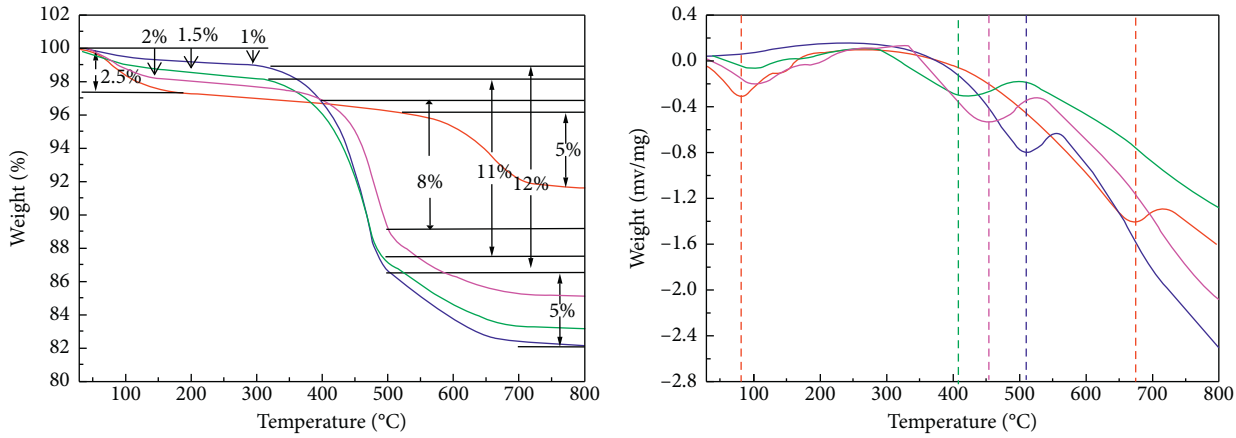

(a) (b)

Figure 2: TG (a) and DTA (b) curves of Na-Mt and C_4-Mt. Na-Mt (red), C_4-Mt-1 (pink), C_4-Mt-2 (green), and C_4-Mt-3 (blue).

which will result in an increase in basal spacing. Based on negative layer charge of Mt, three Al atoms were replaced by Mg atoms in 12 unit cells during the process of simulation construction, leaving a layer charge of −3 counterbalanced by three Na^+. According to the simulation results (Figure 3(a)), there are two water molecules around every Na^+ in the interlayer with oxygen atoms towards Na^+. The distances between each water molecule and Na^+ are not the same [40, 41]; for example, Na^+ on the left side, one of the Na^+–O distance is 2.192 Å while the other one is 3.786 Å. A similar result can be drawn from the other two Na^+: for the distances between water molecules and Na^+, there is always one <2.5 Å and one >3 Å. The force between two atoms is inversely associated with the distance between them. The stronger the electrostatic force is, the shorter the distance between two atoms will be. Apart from that, the force existed between Na^+ and oxygen of the six oxygen rings of the silicon-oxygen tetrahedron. The shortest distance between Na^+ and oxygen in silicon-oxygen tetrahedron is 2.423 Å, 2.356 Å, and 2.264 Å, respectively. Na-Mt has a basal spacing of 12.34 Å with a layer thickness of 9.8 Å, so the space for $Na{\cdot}H_2O^+$ should be 2.54 Å (12.34–9.8). Because the shortest distance between Na^+ and the surface of silicon-oxygen tetrahedron is 1.545 Å, there should be one layer of $Na{\cdot}H_2O^+$ in the middle of Mt. It can be found that all three Na^+ ions are distributed on top of the six oxygen rings of silicon-oxygen tetrahedron and are closer to the Mg position because the negative charge caused by ion substitution in the octahedron layer increases the electric field and results in an increase in electrostatic energy for Na^+ (Figure 3(b)). To sum up, Na^+ in the interlayer of Mt can form hydrated cations with water molecules, and some of them can form relatively weak bond with the oxygen in the silicon-oxygen tetrahedron, which means Na-Mt is exchangeable.

3.3. Simulation of the Intercalation Process of Mt by Organic Cations. The order that the three Na^+ in Mt exchanged by C_4mim^+ related to the free energy between Na^+ and silicon-oxygen tetrahedron. The closest distance between Na^+ on the right (Na^+-1) and oxygen of silicon-oxygen tetrahedron is 2.423 Å (Figure 3(a)), which is the longest one. Because longer distance means weaker free energy between them, Na^+ on the right got exchanged firstly during the intercalation. The water around that Na^+ was also exchanged leaving out only C4mim$^+$ in the place. Because the closest distance between Na^+ in C_4mim^+ and oxygen in the silicon-oxygen tetrahedron is 3.834 Å (Figure 4(a)), which is too long to form any chemical bond, C_4mim^+ is arranged parallel to the layer, and the basal spacing of Mt is increased by 0.38 Å to 12.72 Å. For the other two Na^+, the closest distance between them and the oxygen in silicon-oxygen tetrahedron turns out to be 2.392 Å and 2.039 Å, which is longer than that before the interaction. This means that more energy will be needed to enable those two Na^+ exchanged by C_4mim^+.

As the intercalation continues, Na^+ (Na^+-2) that has a closest distance to the oxygen in silicon-oxygen tetrahedron of 2.356 Å was exchanged next (Figure 4(b)) and Na^+ (Na^+-3) with the shortest distance to the oxygen in silicon-oxygen tetrahedron was exchanged last (Figure 4(b)). The shorter the distance between Na^+ and silicon-oxygen tetrahedron is, the stronger the free energy was between them, and the more difficult it can be for ion exchange. The closest distances between C_4mim^+ in places of Na^+-2 and Na^+-3 with oxygen in silicon-oxygen tetrahedron are 3.742 Å and 3.493 Å, respectively. Besides, the free energy between them is very weak. When Na^+-2 and Na^+-3 were exchanged, the basal spacing of Mt was increased to 13.11 Å. And the basal spacing turns out to be 13.43 Å after all of Na^+ were exchanged, which is consistent with the XRD result that basal spacing of Mt increases as the amount of C_4mim^+ intercalated increases. When all Na^+ were exchanged, the closest distance between three C_4mim^+ and oxygen in silicon-oxygen tetrahedron is 4.633 Å, 4.057 Å, and 3.589 Å, respectively (Figure 4(c)), which were all larger than 2.5 Å and larger than that when the first two C_4mim^+ were intercalated (Figures 4(a) and 4(b)). C_4mim^+ has a very weak interaction with the structure layer and cannot form bonds with oxygen in silicon-oxygen tetrahedron. They arranged as a single layer in the interlayer region parallel to the

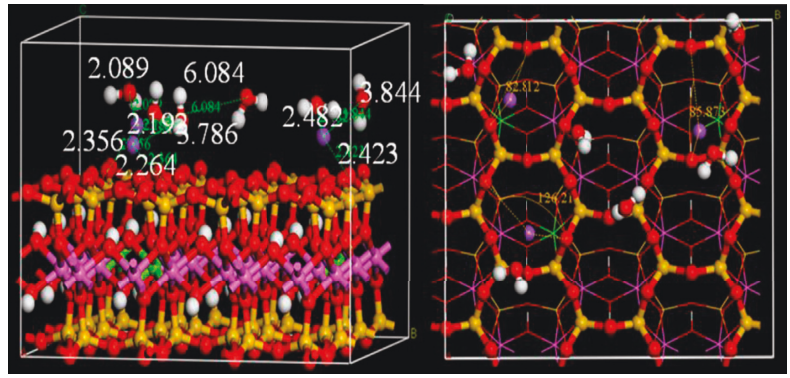

Figure 3: Molecular dynamic simulation of the distance of Na^+ with [SiO_4]. For all species, C = gray, N = blue, H = white, O = red, Si = yellow, Na = purple, Al = pink, and Mg = green.

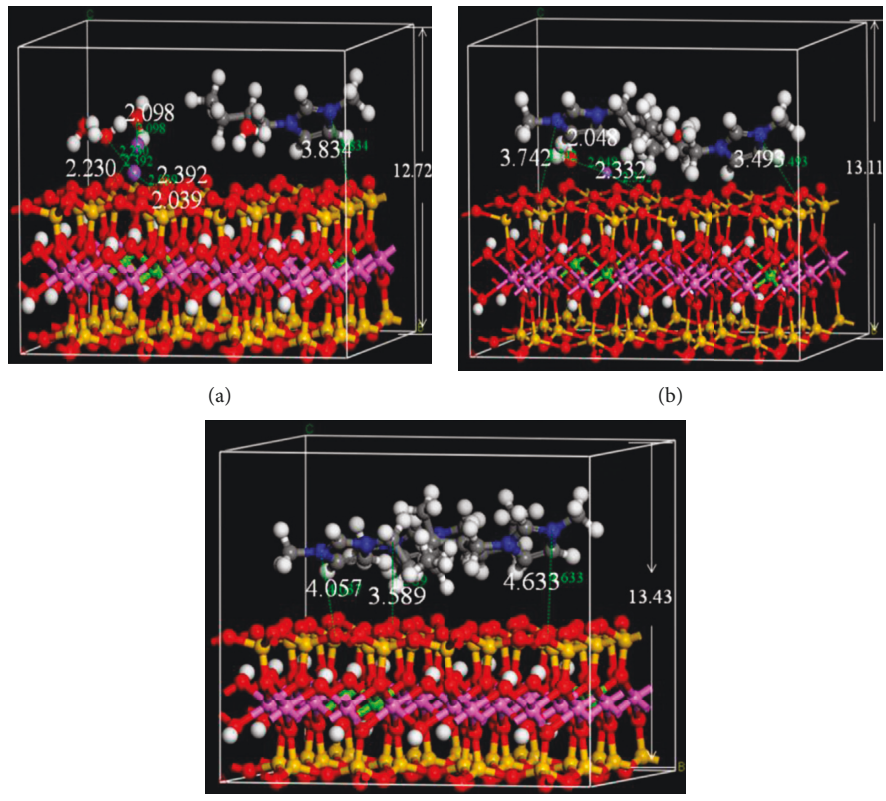

(a) (b)

(c)

Figure 4: Molecular dynamic simulation of the distance of Na^+ and C_4mim^+ with [SiO_4].

structure layer in the interlayer region. Cations in the interlayer of Mt exchanged under the action of external mechanical energy, and the energy of C_4mim^+ keeps changing during intercalating Mt (Table1), which indicates the stability of the structure. As the amount of the intercalated cations increases, the energy keeps increasing, Mt-3C_4 (−866 eV) > Mt-2C_4 (−547 eV) > Mt-1C_4 (−221 eV), and the basal spacing increases. As we know, the lower the energy is, the more stable the structure will be, and the more uniform the distribution of C_4mim^+ will be [13, 42, 43].

Table 1: Interaction energies of four kinds of the intercalation model of C_4mim^+.

Model	d_{001} (Å)	$\triangle E$ (eV)
C_4-Mt-1	12.72	−221
C_4-Mt-2	13.11	−547
C_4-Mt-3	13.43	−866

In Section 3.1, it was established in the DTA discussion that Mt becomes hydrophobic after being intercalated with C_4mim^+, and there were no free water molecules in the

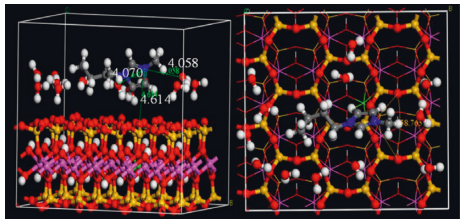

Figure 5: Molecular dynamic simulation of the distance of C_4mim^+ with $[SiO_4]$.

interlayer after the drying process at low temperature. However, the intercalation of Mt with organic cations occurs in solution, which means that water molecules can enter the interlayer of Mt and interact with C_4mim^+ (Figure 5). So interaction between C_4mim^+ and water deserves further discussion. The samples were dried at 60°C before TGA, and the loss of water that coordinates cations for Na-Mt and C_4-Mt are totally different, indicating that water interacts with them differently. In order to determine the hypothesis above, a simulation was conducted. To simplify the model, one C_4mim^+ with 10 water molecules around was arranged in the interlayer of Mt to simulate the state in solution and to investigate the interaction between C_4mim^+ and water molecules. The closest distance between N^+ in C_4mim^+ and oxygen in silicon-oxygen tetrahedron is 4.614 Å. Thus, C_4mim^+ cannot form a chemical bond with oxygen in silicon-oxygen tetrahedron. The interaction between C_4mim^+ and water molecules is also weak because the closest distance between N^+ in C_4mim^+ and oxygen in water molecules is 4.058 Å. The result is totally different with Na-Mt in which chemical bonds can be formed between Na^+ and water into hydration cations (Figure 3). And the distance between alkyl chain in C_4mim^+ and oxygen in water is more than 5 Å, weakly force with water. The intercalation with organic cations can change the interlayer of Mt into the organic environment and change it into hydrophobic from hydrophilic.

4. Conclusions

In conclusion, there are Na^+ ions with three energy states in Mt gallery, which affect the order of organic cations intercalating and their position in gallery. XRD and TG-DTA were undertaken to characterize the change in basal spacing and thermal stability of Mt. During the intercalation, the interaction between original cations and structure layer of Mt keeps changing, and the basal spacing of Mt keeps increasing until an organic environment has been built in the interlayer (increased from 12.34 Å to 14.25 Å). Na^+ ions with the higher energy state are more difficult to be exchanged, and organic cations enter gallery in three steps to occupy the positions of three kinds of Na^+ ions; intercalated organic cations are not bonded with oxygen in silica tetrahedron while locate stably above the hexatomic ring in tetrahedron (above octahedron that aluminum replaced by magnesium); organic cations intercalated latter have higher stability; no interlayer bonding water in organic intercalated Mt, rendering a stronger hydrophobicity than original Mt. The role of energy state of Mt interlayer cations in influencing organic intercalation and its mechanism is significant in preparation and application of organic Mt composite materials.

Data Availability

All data included in this study are available upon request by contacting the corresponding author.

Conflicts of Interest

The authors declare that they have no conflicts of interest.

Acknowledgments

This research was jointly supported by the National Natural Science Foundation of China (51604248 and 51508344), China Postdoctoral Science Foundation funded project (2018M631818), and the Doctoral Startup Foundation of Liaoning (20170520315).

References

[1] T. Vanorio, M. Prasad, and A. Nur, "Elastic properties of dry clay mineral aggregates, suspensions and sandstones," *Geophysical Journal International*, vol. 155, no. 1, pp. 319–326, 2003.

[2] R. Yi, G. Qiu, and X. Liu, "Rational synthetic strategy: from ZnO nanorods to ZnS nanotubes," *Journal of Solid State Chemistry*, vol. 182, no. 10, pp. 2791–2795, 2009.

[3] G. R. Whittell and I. Manners, "Metallopolymers: new multifunctional materials," *Advanced Materials*, vol. 19, no. 21, pp. 3439–3468, 2007.

[4] F. Fang, H. J. Choi, and J. Joo, "Conducting polymer/clay nano composites and their applications," *Journal of Nanoscience and Nanotechnology*, vol. 8, no. 4, pp. 1559–1581, 2008.

[5] Y. F. Xi, R. L. Frost, H. He, T. Kloprogge, and T. Bostrom, "Modification of Wyoming montmorillonite surfaces using a cationic surfactant," *Langmuir*, vol. 21, no. 19, pp. 8675–8680, 2005.

[6] H. P. He, J. F. Galy, and J.-F. Gerard, "Molecular simulation of the interlayer structure and the mobility of alky chains in $HDTMA^+$/montmorillonite hybrids," *Journal of Physical Chemistry B*, vol. 109, no. 27, pp. 13301–13306, 2005.

[7] H. Othmani-Assmann, M. Benna-Zayani, S. Geiger et al., "Physico-chemical characterizations of tunisian organophilic bentonites," *Journal of Physical Chemistry C*, vol. 111, no. 29, pp. 10869–10877, 2007.

[8] B. Ha and K. Char, "Conformational behavior of dodecyldiamine inside the confined space of montmorillonites," *Langmuir*, vol. 21, no. 18, pp. 8471–8477, 2005.

[9] H. P. He, J. Duchet, J. Galy, and J.-F. Gerard, "Grafting of swelling clay materials with 3-aminopropyltriethoxysilane," *Journal of Colloid and Interface Science*, vol. 288, no. 1, pp. 171–176, 2005.

[10] S. J. Chipera and D. L. Bish, "Baseline studies of the clay minerals society source clays: powder X-ray diffraction analyses," *Claysand Clay Minerals*, vol. 49, no. 5, pp. 398–409, 2001.

[11] D. Borden and R. F. Giese, "Baseline studies of the clay minerals society source clays: cation exchange capacity measurements by the ammonia-electrode method," *Clays and Clay Minerals*, vol. 49, no. 5, pp. 444-445, 2001.

[12] F. Bergaya, B. K. G. Theng, and G. Lagaly, "Chapter 10 clays in industry," *Developments in Clay Science*, vol. 1, p. 499, 2006.

[13] X. Liu, X. C. Lu, R. Wang, H. Zhou, and S. Xu, "Molecular dynamics insight into the cointercalation of hexadecyltrimethylammonium and acetate ions into smectites," *American Mineralogist*, vol. 94, no. 1, pp. 143–150, 2009.

[14] H. P. He, J. Duchet, J. Galy, and J.-F. Gérard, "Influence of cationic surfactant removal on the thermal stability of organoclays," *Journal of Colloid and Interface Science*, vol. 295, no. 1, pp. 202–208, 2006.

[15] X. Y. Wen, H. P. He, J. Zhu, Y. Jun, C. Ye, and F. Deng, "Arrangement, conformation, and mobility of surfactant molecules intercalated in montmorillonite prepared at different pillaring reagent concentrations as studied by solid-state NMR spectroscopy," *Journal of Colloid and Interface Science*, vol. 299, no. 2, pp. 754–760, 2006.

[16] A. R. Mermut and G. Lagaly, "Baseline studies of the clay minerals society source clays: layer-charge determination and characteristics of those minerals containing 2 : 1 layers," *Clays and Clay Minerals*, vol. 49, no. 5, pp. 393–397, 2001.

[17] G. C. Lv, C. W. Pearce, A. Gleason, L. Liao, M. P. MacWilliams, and Z. Li, "Influence of montmorillonite on antimicrobial activity of tetracycline and ciprofloxacin," *Journal of Asian Earth Sciences*, vol. 77, pp. 281–286, 2013.

[18] L. M. Wu, L. B. Liao, G. Lv, F. Qin, and Z. Li, "Microstructure and process of intercalation of imidazolium ionic liquids into montmorillonite," *Chemical Engineering Journal*, vol. 236, pp. 306–313, 2014.

[19] H. Heinz and U. W. Suter, "Surface structure of organoclays," *Angewandte Chemie International Edition*, vol. 43, no. 17, pp. 2239–2243, 2004.

[20] J. Wang, A. G. Kalinichev, R. J. Kirkpatrick, and R. T. Cygan, "Structure, energetic and dynamics of water adsorbed on the muscovite (001) surfaces: a molecular dynamics simulation," *Journal of Physical Chemistry B*, vol. 109, no. 33, pp. 15893–15905, 2005.

[21] H. Heinz, R. A. Vaia, R. Krishnamoorti, and B. L. Farmer, "Self-assembly of alkylammonium chains on montmorillonite: effect of chain length, head group structure, and cation exchange capacity," *Journal of Materials Chemistry*, vol. 19, no. 1, pp. 59–68, 2007.

[22] V. Marry, B. Rotenberg, and P. Turq, "Structure and dynamics of water at a clay surface from molecular dynamics simulation," *Physical Chemistry Chemical Physics*, vol. 10, no. 32, pp. 4802–4813, 2008.

[23] R. T. Cygan, "Molecular modeling in mineralogy and geochemistry," *Reviews in Mineralogy and Geochemistry*, vol. 42, no. 1, pp. 1–35, 2001.

[24] M. Arab, D. Bougeard, and K. S. Smirnov, "Structure and dynamics of interlayer species in a hydrated Zn-vermiculite. A molecular dynamics study," *Physical Chemistry Chemical Physics*, vol. 6, no. 9, pp. 2446–2453, 2004.

[25] Y. Ichikawa, K. Kawamura, N. Theramast, and K. Kitayama, "Secondary and tertial consolidation of bentonite clay: consolidation test, molecular dynamics simulation and multiscale homogenization analysis," *Mechanics of Materials*, vol. 36, no. 5-6, pp. 487–513, 2004.

[26] S. Satoru and K. Katsuyuki, "Study of vibrational spectra of interlayer water in sodium beidellite by molecular dynamics simulations," *Journal of Physical Chemistry B*, vol. 108, no. 35, pp. 13468–13474, 2004.

[27] H. C. Greenwell, L. A. Bindley, P. R. Unwin et al., "In situ monitoring of crystal growth and dissolution of oriented layered double-hydroxide crystals immobilized on silicon," *Journal of Crystal Growth*, vol. 294, no. 1, pp. 53–59, 2006.

[28] P. P. Kumar, A. G. Kalinichev, and R. J. Kirkpatrick, "Hydration, swelling, interlayer structure, and hydrogen bonding in organolayered double hydroxides: insights from molecular dynamics simulation of citrate-intercalated hydrotalcite," *Journal of Physical Chemistry B*, vol. 110, no. 9, pp. 3841–3844, 2006.

[29] J. W. Wang, A. G. Kalinichev, and R. J. Kirkpatrick, "Effects of substrate structure and composition on the structure, dynamics, and energetics of water at mineral surfaces: a molecular dynamics modeling study," *Geochimica et Cosmochimica Acta*, vol. 70, no. 3, pp. 562–582, 2006.

[30] T. Kwolek, M. Hodorowicz, K. Stadnicka, and J. Czapkiewicz, "Adsorption isotherms of homologous alkyldimethylbenzylammonium bromides on sodium montmorillonite," *Journal of Colloid and Interface Science*, vol. 264, no. 1, pp. 14–19, 2003.

[31] L. M. Zhou, H. Chen, X. Jiang et al., "Modification of montmorillonite surfaces using a novel class of cationic gemini surfactants," *Journal of Colloid and Interface Science*, vol. 332, no. 1, pp. 16–21, 2009.

[32] B. F. Ngouana and A. G. Kalinichev, "Structural arrangements of isomorphic substitutions in smectites: molecular simulation of the swelling properties, interlayer structure, and dynamics of hydrated Cs–Montmorillonite revisited with new clay models," *Journal of Physical Chemistry C*, vol. 118, no. 24, pp. 12758–12773, 2014.

[33] R. Ait-Akbour, P. Boustingorry, F. Leroux, F. Leising, and C. Taviot-Guého, "Adsorption of Poly Carboxylate Poly (ethylene glycol) (PCP) esters on Montmorillonite (Mmt): effect of exchangeable cations (Na^+, Mg^{2+} and Ca^{2+}) and PCP molecular structure," *Journal of Colloid and Interface Science*, vol. 437, pp. 227–234, 2015.

[34] J. Greathouse and R. T. Cygan, "Water structure and aqueous uranyl(VI) adsorption equilibria onto external surfaces of beidellite, montmorillonite, and pyrophyllite: results from molecular simulations," *Environmental Science and Technology*, vol. 40, no. 12, pp. 3865–3871, 2006.

[35] V. Aggarwal, Y. Y. Chien, and B. J. Teppen, "Molecular simulations to estimate thermodynamics for adsorption of polar organic solutes to montmorillonite," *European Journal of Soil Science*, vol. 58, no. 4, pp. 945–957, 2007.

[36] K. F. Austen, T. O. H. White, A. Marmier, S. C. Parker, E. Artacho, and M. T. Dove, "Electrostatic versus polarization effects in the adsorption of aromatic molecules of varied polarity on an insulating hydrophobic surface," *Journal of Physics: Condensed Matter*, vol. 20, no. 3, pp. 203–215, 2008.

[37] R. Zhu, T. V. Shapley, M. Molinari, G. Fei, and S. C. Parker, "Structure of water saturated CTMA-montmorillonite hybrid: molecular dynamics simulation investigation," *Advances in Materials Research*, vol. 233-235, pp. 1372–1877, 2011.

[38] G. K. Zhang, Y. Y. Gao, Y. Zhang, and Y. Guo, "Fe_2O_3-Pillared rectorite as an efficient and stable fenton-like heterogeneous catalyst for photodegradation of organic contaminants," *Environmental Science & Technology*, vol. 44, no. 16, pp. 6384–6389, 2010.

[39] F. Piscitelli, P. Posocco, R. Toth et al., "Sodium montmorillonite silylation: unexpected effect of the aminosilane chain length," *Journal of Colloid and Interface Science*, vol. 351, no. 1, pp. 108–115, 2010.

[40] L. M. Wu, L. B. Liao, and G. Lv, "Influence of interlayer cations on organic intercalation of montmorillonite," *Journal of Colloid and Interface Science*, vol. 454, pp. 1–7, 2015.

[41] Y. Xu, Y. Liu, D.-D. He, and G.-S. Liu, "Adsorption of cationic collectors and water on muscovite (001) surface: a molecular dynamics simulation study," *Minerals Engineering*, vol. 53, pp. 101–107, 2013.

[42] A. M. Shanmugharaj, K. Y. Rhee, and S. H. Ryu, "Influence of dispersing medium on grafting of aminopropyltriethoxysilane in swelling clay materials," *Journal of Colloid and Interface Science*, vol. 298, no. 2, pp. 854–859, 2006.

[43] F. Q. Dong, L. Bian, M. Song, W. Li, and T. Duan, "Computational investigation on the fn → fn−1d effect on the electronic transitions of clinoptilolite," *Applied Clay Science*, vol. 119, pp. 74–81, 2016.